Title	Plasmonic optical trap having very large active volume realized with nano-ring structure
Author(s)	Kang, Zhiwen; Zhang, Haixi; Lu, Haifei; Xu, Jianbin; Ong, Hock-Chun; Shum, Perry Ping; Ho, Ho-Pui
Citation	Kang, Z., Zhang, H., Lu, H., Xu, Ji., Ong, H.-C., Shum, P., et al. (2012). Plasmonic optical trap having very large active volume realized with nano-ring structure. Optics Letters, 37(10), 1748-1750.
Date	2012
URL	http://hdl.handle.net/10220/10974
Rights	© 2012 Optical Society of America. This paper was published in Optics Letters and is made available as an electronic reprint (preprint) with permission of Optical Society of America. The paper can be found at the following official DOI: [http://dx.doi.org/10.1364/OL.37.001748]. One print or electronic copy may be made for personal use only. Systematic or multiple reproduction, distribution to multiple locations via electronic or other means, duplication of any material in this paper for a fee or for commercial purposes, or modification of the content of the paper is prohibited and is subject to penalties under law.

Plasmonic optical trap having very large active volume realized with nano-ring structure

Zhiwen Kang,[1] Haixi Zhang,[1] Haifei Lu,[1] Jianbin Xu,[1] Hock-Chun Ong,[2] Ping Shum,[3] and Ho-Pui Ho[1,*]

[1]*Department of Electronic Engineering, The Chinese University of Hong Kong, Shatin, NT, Hong Kong SAR, China*

[2]*Department of Physics, The Chinese University of Hong Kong, Shatin, NT, Hong Kong SAR, China*

[3]*OPTIMUS—Photonics Centre of Excellence, School of Electrical and Electronic Engineering, Nanyang Technological University, 50 Nanyang Avenue, Singapore*

**Corresponding author: hpho@ee.cuhk.edu.hk*

Received December 16, 2011; revised February 27, 2012; accepted March 1, 2012; posted March 2, 2012 (Doc. ID 160138); published May 15, 2012

The feasibility of using gold nano-rings as plasmonic nano-optical tweezers is investigated. We found that at a resonant wavelength of $\lambda = 785$ nm, the nano-ring produces a maximum trapping potential of $\sim 32 k_B T$ on gold nanoparticles. The existence of multiple potential wells results in a very large active volume of $\sim 10^6$ nm^3 for trapping the target particles. The report nano-ring design provides an effective approach for manipulating nano-objects in very low concentration into the high-field region and is well suited for integration with microfluidics for lab-on-a-chip applications.

OCIS codes: 240.6680, 350.4855.

Plasmonic nano-optical tweezers (PNOTs) have attracted much research interest recently because of their ability to immobilize nano-sized objects with ultrahigh accuracy, thus showing potential applications in chemo- and biosensing and life sciences [1,2]. Optical trapping strength is dictated primarily by the depth of the trapping potential well associated with the field intensity gradient, which is further aided by localized surface plasmons (LSP) [1–4]. Until now, PNOTs based on metal dipole antennas [2,3], thin films [5], sharp tips [6], cavities [7], holes [8], disks [9,10], and hybrid waveguides [11] have been realized theoretically and/or experimentally. However, to the best of our knowledge, there is no report on optical trapping using metal nano-rings despite that they may offer performance merits including polarization-insensitive characteristics, widely tunable resonance, strong and uniform field enhancement around and inside the ring cavity, and ease of fabrication [12,13].

In addition, gold nanoparticles (Au-NPs) are widely adopted as optical signal enhancement agents due to their plasmonic resonance and various chemical functionalization possibilities. Hence, trapping and immobilizing Au-NPs to a predefined region of high sensitivity plays an important role in achieving high detection signal levels. It has been reported that 10 nm Au-NPs can be trapped inside the gap of a plasmonic dipole antenna, and the trapping effect is monitored by measuring the shift of Rayleigh scattering [3]. This kind of PNOT provides a detection limit in the particles' size of 5 nm for plasmonic NPs and 6.5 nm for dielectric NPs [14]. However, the active trap volume is small due to the narrow gap used [3,14]. In this Letter, we demonstrate a new kind of PNOT based on gold nano-ring array for three-dimensional (3D) optical trapping of Au-NPs. Results obtained using 3D finite-difference time-domain (FDTD) simulation [15] and the Maxwell stress tensor (MST) [5,11] indicate that the nano-ring PNOT exhibits strong trapping potential well and very large active volume, and thus is effective for bringing NPs that are of low concentrations into the high-field region. The device has strong application potential in the field of biodetection and molecular spectroscopy.

Figure 1(a) shows the structure of the proposed gold nano-ring. The overall device is in a two-dimensional array format so that resonance modes also occur between nano-ring elements and many optical traps may be energized simultaneously with a focused laser spot. The structural parameters are periodicity L, thickness t, and inner and outer diameters D_1 and D_2, respectively. Note that the origin of the coordinate has been offset to the left corner for clarity and is actually located at the ring center and the substrate (SiO_2, $n = 1.5$) surface. The environment is water ($n = 1.33$) containing free Au-NPs. In our simulation study, periodic boundary conditions are used in the x and y directions, and perfect matching layers in the z direction. The relative permittivity of Au is based on reported experimental data [16]. The light source is a plane wave illuminating from the top along the normal direction with electric field (amplitude 1 V/m) polarized along the x axis.

Figure 1(b) shows typical extinction (solid curve) and electric field intensity (E^2, dotted curve) spectra at the nano-ring edge [marked by a black dot in Fig. 1(a)] as appropriate structural parameters are chosen, namely, $D_1 = 40$ nm, $D_2 = 100$ nm, $t = 35$ nm, and $L = 525$ nm in order to produce a narrow dominating resonance peak at $\lambda = 785$ nm because of the excitation of LSPs and plasmonic interference within the nano-ring array [17]. The edges have been rounded to a radius of 4 nm. Actually

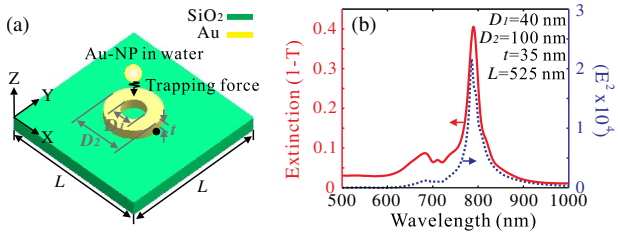

Fig. 1. (Color online) (a) Schematic of one unit cell of the gold nano-ring arrays. (b) Extinction (solid curve) of the nano-ring arrays and the E^2 spectrum (dotted curve) of the nano-ring edge as indicated by a black dot in Fig. 1(a). Dimensions of nano-ring: $D_1 = 40$ nm, $D_2 = 100$ nm, $t = 35$ nm, and $L = 525$ nm.

the resonance can be readily tuned by varying the dimensional parameters. Increasing the diameters (or ring width) or reducing the device thickness or corner sharpness will redshift the resonance, and vice versa (data not shown). The choice of 785 nm is due to the availability of commercial laser sources and relative lower plasmonic energy dissipation as compared to visible wavelengths. Moreover, the chosen parameters have also taken into account typical fabrication constraints [12,13].

We next use the MST to calculate the trapping forces experienced by the NP due to enhanced local field. Figure 2(a) shows the spectra of vertical forces F_z acting on a Au-NP (solid curve) and a polystyrene sphere (PS; $n = 1.6$, dotted curve, magnified 10 times) as a function of incident wavelength. PS provides a reference case for quantifying the contribution of plasmonic effects. The data have been normalized to incident intensity and illumination area. The NPs used in this case have a diameter of 20 nm and are located at $(0, 0, 35)$ nm (marked by black dot). One can see that F_z increases significantly when the wavelength changes towards resonance at $\lambda = 785$ nm. The Au-NP experiences a maximum vertical force F_z as high as 236 pN/W/μm^2, which is ~15 times larger than that seen by the PS because of higher polarizability of gold [3,4,11]. The negative sign of F_z is consistent with the trapping nature of F_z along the $-z$ direction. The other force components F_x and F_y are zero due to symmetry of the structure.

To examine the spatial distribution of the trapping force, we fix the wavelength at $\lambda = 785$ nm. Figure 2(b) shows the spectra of F_z experienced by the Au-NP (circles) and the PS (squares, magnified 10 times) as a function of location along the z axis ($x = y = 0$), and the gradient of electric field intensity along this direction ($\partial E^2/\partial z$) (dotted curve). Consistent with previous results, the PS NP experiences smaller trapping force. Obviously, excellent correlation occurs between the electric field intensity gradient and F_z because of the fact that trapping force is proportional to the gradient of E^2 ($F = -C\nabla E^2$, with coefficient C taking into account the NP's polarizability and the surrounding refractive index) [4,11]. At $z = 38$ nm the gradient is at its maximum, indicating that this is the location of highest F_z. At $z = 17.5$ nm, both the gradient and F_z return to zero, followed by a change of sign from "−" to "+" for the region of $z < 17.5$ nm. This means that the NP will be trapped slightly above the substrate surface.

In order to calculate the effective trapping strength, we find the trapping potential U experienced by the Au-NP at a distance r_o using $U = -\int_{\infty}^{r_0} F(r)dr$ [4,6,11]. At $z = 38$ nm, the trapping force is 265 pN/W/μm^2, which corresponds to a trapping potential of 4.4×10^{-17} J/W/μm^2. If one uses a low laser power density such as 1 mW/μm^2, the trapping potential will be 4.4×10^{-20} J, which is ~11 times larger than the kinetic energy of Brownian motion ($k_BT = 4.1 \times 10^{-21}$ J at room temperature, where k_B is the Boltzmann constant and T is absolute temperature). For $z = 17.5$ nm, the optically induced potential well reaches a depth of ~$32k_BT$, which is 5.3 times larger than that of a dipole antenna [3]. This result further confirms our expectation that the proposed nano-ring design is effective for performing practical trapping of NPs.

Because trapping forces are primarily due to optical localization, they naturally occur at the corners of the nano-ring [12]. Here we study the trapping force distribution along several directions around the surface of the nano-ring to find the locations where the Au-NP will undergo the strongest trapping potential. The first path is along the axis of $(x, 0, 50)$ nm as indicated by a thick solid arrow in Fig. 3(a). The variations of F_x (circles) and F_z (squares) as a function of location along this axis are shown in Fig. 3(a). We see that F_x becomes zero at $x = 47$ nm and positive for 0 nm $< x <$ 47 nm, but negative for $x > 47$ nm. On other words, F_x changes sign when the Au-NP moves across the top surface of the nano-ring. The fact the $F_x = 0$ at $x = 47$ nm means that naturally the Au-NP will be driven to this location as soon as it falls into the trapping zone. On the other hand, as F_z remains negative for most of this path, the Au-NP also experiences a downward (trapping) force towards the $-z$ direction. This means that any free Au-NP in the vicinity of the top surface of the nano-ring, the combined effect of F_x and F_z will produce a stable trapping site near the outer corner on the top surface, as indicated by a black dot in the cross-section shown in Fig. 3(a). For other regions

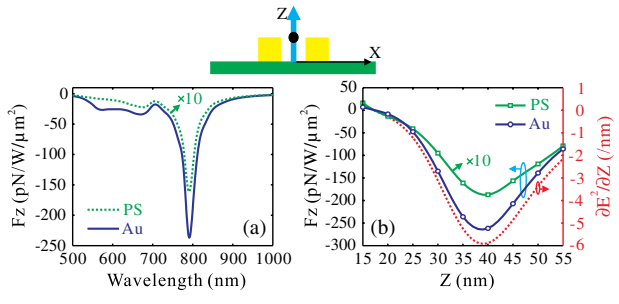

Fig. 2. (Color online) (a) F_z acting on the Au-NP (solid curve) and the PS (dotted curve, magnified 10 times) as a function of incident wavelength. Both NPs have a diameter of 20 nm and are located at coordinates of $(0, 0, 35)$ nm as indicated by a dark dot in the cross-section schematic. (b) Spectra of F_z on the Au-NP (circles) and the PS (squares, magnified 10 times) as a function of position along the z axis ($x = y = 0$) and the electric field intensity gradient along this axis (dotted curve), respectively. Excitation wavelength: 785 nm.

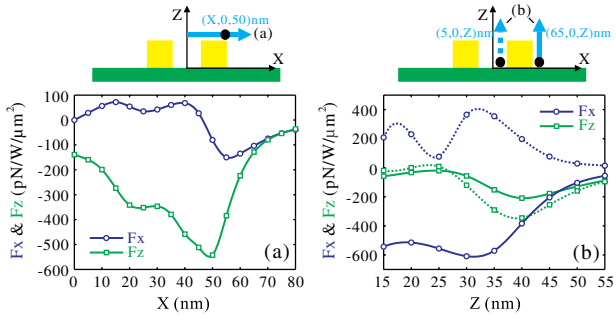

Fig. 3. (Color online) (a) Spectra of F_x (circles) and F_z (squares) as a function of location along the axis of $(x, 0, 50)$ nm (indicated by thick arrow in cross-section schematic). (b) Spectra of F_x and F_z as a function of position along the axes of $(65, 0, z)$ nm (indicated by thick solid arrow) (circles for F_x and squares for F_z), and $(5, 0, z)$ nm (indicated by thick dotted arrow) (dotted curve with circles for F_x and dotted curve with squares for F_z), respectively. The incident wavelength is 785 nm.

around the nano-ring the Au-NP will be trapped by other sites near the substrate surface.

The other two paths are along the axes of $(65, 0, z)$ nm and $(5, 0, z)$ nm as indicated in Fig. 3(b) by the thick solid and dotted arrows. The variations of F_x (solid and dotted curves with circles) and F_z (solid and dotted curves with squares) as a function of location along the two axes are also shown in Fig. 3(b). Note that solid curves correspond to the $(65, 0, z)$ case, while the dotted curves correspond to the $(5, 0, z)$ case. One can see that any Au-NP travelling along these two axes will experience a maximum F_z at 5 nm above the nano-ring (i.e., $z = 40$ nm) and be pulled towards the substrate (i.e., negative F_z). On the other hand, F_x is negative for the case of $(65, 0, z)$ (solid circles) but positive for $(5, 0, z)$ (dotted circles), which suggests that the Au-NP will be driven towards the edge of the nano-ring until the two finally make contact with each other. The overall effect of F_x and F_z is to bring the Au-NP to the bottom corners if it arrives at any location below the top surface of the nano-ring (i.e., $z < 35$ nm). These trapping locations are highlighted by two black dots in Fig. 3(b).

Because the nano-ring has multiple trapping zones as revealed in the above analysis, the total volume as well as surface area of the final optical trap will be enlarged substantially. For example, for any Au-NP at a distance of 30 nm from the nano-ring [see Fig. 3(a), $x = 80$ nm], it will experience a strong trapping force of 40 pN/W/μm^2, which corresponds to a trapping potential of 4.8×10^{-21} J with an incident power density of 1 mW/μm^2. This is still larger than the kinetic energy of the Brownian motion. If we define the trapping boundary as $|U| = k_B T$ [4], that is, trapping potential having the same value as the Brownian motion, and the Au-NP can be trapped by the nano-ring whenever it is within the range of $|U| > k_B T$, we can readily obtain the size of the trapping volume. Figure 4 shows the electric field distribution in the xz plane and the calculated trapping boundary (white circles). The trapping volume, which takes a symmetric shape for the structure considered, is of the order 10^6 nm^3. This is 10^4 and 10^2 times larger than those of the silver nanoaggregates ($\sim$100 nm^3) [4] and dipole antennas ($\sim 10^4$ nm^3) [3,14] respectively. Such large active volume is very attractive for low-concentration operation as the trapping probability of NPs will be increased significantly. While trapping of a single Au-NP within a volume of 0.1 to 1 μm^3 has been reported previously [3], the large active volume from our nano-ring therefore may offer single Au-NP trapping a very low concentration of $10^{-11}\sim 10^{-12}$ mol/L. Potential applications including NP (or biomolecule-functionalized Au-NP) manipulation or detection with single-molecule sensitivity may become possible. Moreover, it is worth mentioning that our emphasis is on trapping of NPs, whereas previous work was mainly concerned with trapping of micro-PSs or yeast cells using microdisks [9,10]. In addition, an array of the proposed nano-rings, apart from being capable of performing parallel trapping of many NPs, can trap micro-objects through a mechanism similar to the antenna case [1].

It is worth pointing out that large active volume always occurs within a wide spectral range as long as the resonance condition is fulfilled (as governed by the choice of dimensional parameters) because the enhanced volume

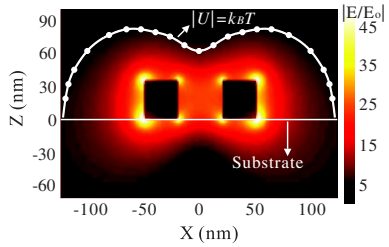

Fig. 4. (Color online) Electric field distribution in the xz plane and the trapping boundary (white circles) $|U| = k_B T$. Excitation wavelength and power density are respectively 785 nm and 1 mW/μm^2.

is essentially due to strong field coupling between the inner and outer surfaces of the nano-ring (see Fig. 4). On the other hand, for antennas or nano-disks of the same size, the field is only localized within the gap or the outer surface without the presence of such coupling effects.

In conclusion, we have numerically demonstrated a gold nano-ring PNOT device operating at $\lambda = 785$ nm for 3D optical trapping of Au-NPs. The device exhibits multiple trapping locations and has a very large active trapping volume of $\sim 10^6$ nm^3, thus providing effective manipulation of nano-objects at very low concentrations into the high-field region and offering application potential in the field of microfluidics and lab-on-a-chip for biodetection.

The authors acknowledge the financial support from RGC General Research Grant #412208, CUHK Group Research project #3110070 and project# BME p3-11 from the Shun Hing Institute of Advanced Engineering. We are also grateful to CUHK for research studentship support of ZWK and HFL.

References

1. M. L. Juan, M. Righini, and R. Quidant, Nat. Photon. **5**, 349 (2011).
2. A. N. Grigorenko, N. W. Roberts, M. R. Dickinson, and Y. Zhang, Nat. Photon. **2**, 365 (2008).
3. W. Zhang, L. Huang, C. Santschi, and O. J. F. Martin, Nano Lett. **10**, 1006 (2010).
4. H. Xu and M. Käll, Phys. Rev. Lett. **89**, 246802 (2002).
5. Y. J. Zheng, H. Liu, S. M. Wang, T. Li, J. X. Cao, L. Li, C. Zhu, Y. Wang, S. N. Zhu, and X. Zhang, Appl. Phys. Lett. **98**, 083117 (2011).
6. B. Liu, L. Yang, and Y. Wang, Opt. Express **19**, 3703 (2011).
7. R. Sainidou and F. J. García de Abajo, Phys. Rev. Lett. **101**, 136802 (2008).
8. M. L. Juan, R. Gordon, Y. Pang, F. Eftekhari, and R. Quidant, Nat. Phys. **5**, 915 (2009).
9. H. M. K. Wong, M. Righini, J. C. Gates, P. G. R. Smith, V. Pruneri, and R. Quidant, Appl. Phys. Lett. **99**, 061107 (2011).
10. L. Huang, S. J. Maerkl, and O. J. F. Martin, Opt. Express **17**, 6018 (2009).
11. X. Yang, Y. Liu, R. F. Oulton, X. Yin, and X. Zhang, Nano Lett. **11**, 321 (2011).
12. J. Aizpurua, P. Hanarp, D. S. Sutherland, M. Käll, G. W. Bryant, and F. J. García de Abajo, Phys. Rev. Lett. **90**, 057401 (2003).
13. M. G. Banaee and K. B. Crozier, Opt. Lett. **35**, 760 (2010).
14. A. Lovera and O. J. F. Martin, Appl. Phys. Lett. **99**, 151104 (2011).
15. D. M. Sullivan, *Electromagnetic Simulation Using the FDTD Method* (IEEE, 2000).
16. P. B. Johnson and R. W. Christy, Phys. Rev. B **6**, 4370 (1972).
17. B. Auquié and W. L. Barnes, Phys. Rev. Lett. **101**, 143902 (2008).